THE DESIGN OF TOUGH FERRITIC CRYOGENIC STEELS

by

J. W. Morris, Jr. and Sungho Jin

Department of Materials Science and Engineering, College of Engineering and Inorganic Materials Research Division, Lawrence Berkeley Laboratory; University of California, Berkeley, California 94720

ABSTRACT

It has long been known that ferritic steels would attain high strength levels at cryogenic temperature because of the pronounced thermal contribution to the yield strength of the BCC structure at low temperature. However, this increase in strength typically induces an embrittlement (the ductile-brittle transition) which severely restricts the utilization of available ferritic steels in cryogenic systems. Recent research has shown that this low-temperature embrittlement may be overcome through a careful matching of composition and microstructure. In the following paper we discuss the microstructural features important in a tough cryogenic steel and illustrate alloy design techniques by describing the processing and properties of two new cryogenic steels, of nominal composition Fe-12Ni-0.25Ti and Fe-8Ni-2Mn-0.25Ti.

I. INTRODUCTION

The need for major engineering advances in the production, transport, and storage of useful energy has brought about an increasing interest in the potential of cryogenic systems. Relevant current problems include the safe transport and storage of liquified gases and the design of advanced engines, power generation facilities, and coal conversion devices utilizing superconducting magnets cooled in liquid helium. Progress in solving these problems will require significant improvements in engineering materials as well as in systems design.

The research described below has focused on one potential materials need: strong, tough alloy steels which retain good properties to 4°K, the ambient temperature of a cooled superconducting magnet. The initial problem which had to be overcome in this research was the "ductile-brittle transition" behavior common to ferritic steels (steels having a matrix based on the ferrite, or body-centered-cubic crystal structure of iron).

As is well known, materials having a body-centered-cubic (BCC) crystal structure show an appreciable increase in strength when tested at low temperature. This "thermal component" of the yield strength of BCC alloys makes ferritic steels particularly attractive for cryogenic use; one may easily make alloys which become very strong at cryogenic service temperatures. However, as the strength of a ferritic alloy increases on cooling the alloy also tends to become brittle, often through a dramatic loss of toughness over a rather narrow temperature range which defines the "ductile brittle transition temperature" (T_B). This low temperature embrittlement severely restricts the use of ferritic alloys

in cryogenic systems. If metallurgical techniques can be employed to overcome low temperature embrittlement in ferritic steels or to suppress T_B to well below service temperatures then it becomes possible to design steels having exceptional combinations of cryogenic strength and toughness.

To control ductile-brittle transition behavior one must begin from some understanding of its causes. While these remain incompletely known, the results of metallurgical research on the determination of ductility by alloy microstructure have revealed several important factors. These concern the nature of the alloy matrix, the nature of the grain boundaries separating adjacent grains, and the size and geometry of grains.

To achieve toughness, the interior of alloy grains should be structured so as to permit the flow of dislocations and resist the build-up of concentrated internal stresses. Such a structure should be free of large precipitate particles which may fracture causing local failure, free of large planar barriers to dislocation glide such as lattice twins, and, at low temperature, substantially free of interstitial species which may form pinning atmospheres about potentially mobile dislocations. The grain boundaries should resist brittle intergranular fracture or tearing, and should not retard the transmission of deformation from grain to grain. The grain boundaries should hence be free of harmful segregants which lower grain boundary energy and should be free of brittle films or precipitates which may cause catastrophic intergranular fracture and retard the accomodation of plastic deformation within grains. The grains themselves should be small and randomly oriented. Fine grain size is beneficial for two reasons.[1] First, should a grain fail through

local cleavage, the size of the resulting flaw is limited by grain size. Since the stress required to locally initiate fracture varies as $c^{-1/2}$, where c is the dimension of the largest local flaw, the local fracture stress tends to vary as $d^{-1/2}$, where d is the mean grain diameter. Secondly, the maximum internal stress at the boundary of a yielded grain tends to increase with the grain size. This stress, due to the pile-up of a series of dislocations pinned by the grain boundary, is expected to be particularly important at low temperature where thermally-activated processes which may relax dislocation pile-ups are relatively ineffective. The stress due to a pile-up increases with the number of dislocations in the pile-up; hence its maximum value increases with grain size (as $d^{1/2}$). In a fine-grained alloy the relative orientation of adjacent grains is also important. If the grains are preferentially aligned with one another they may cooperatively provide easy paths for crack propagation.

The considerations above suggest desirable microstructural characteristics for a steel to be both strong and tough at low temperature. This desirable microstructure can be obtained through a favorable choice of alloy composition and processing, as described in the following.

II. DESIGN OF A CRYOGENIC STEEL

The design of an alloy begins with a choice of nominal composition. In the present work we sought alloys which maximize strength and ductility at cryogenic temperature, and hence wished to obtain a BCC alloy whose native microstructure would be favorable to low-temperature deformation. Iron-nickel alloys of intermediate nickel content (8-20% nickel by weight) are particularly promising. On quenching, Fe-Ni alloys of this

composition transform to a lathe-like BCC martensite which is heavily dislocated and almost free of transformation strains (Fig. 1). This microstructure contains a dense array of potentially mobile dislocations and provides a favorable matrix for dislocation flow. In choosing alloys of the Fe-Ni series, economic considerations argue that the nickel content should be kept as low as possible. Our research has concentrated on Fe-12Ni and Fe-8Ni alloys.

Low temperature toughness further requires that the alloy be purified of grain boundary segregants which may cause embrittlement and of unwanted interstitials which may form pinning atmospheres about dislocations. This purification may be accomplished by using purified starting materials, by employing advanced melting or remelting techniques, or by incorporating chemical species which "getter" unwanted impurities into relatively innocuous precipitates. In industrial practice a combination of melting technique (vacuum induction melting (VIM), vacuum arc remelting (VAR) or electroslag remelting (ESR)) and "gettering" additions is usually used. In laboratory research we employed purified starting materials, melted in inert gas atmosphere, and used a small titanium addition (0.25-0.5 wt.%) to getter residual carbon and oxygen impurities. The titanium also gives a fine precipitate of Ni_3Ti distributed through the microstructure (Fig. 2) which contributes a small increase in the yield strength of the alloy.

Low temperature toughness next requires that the alloy be grain-refined. Metallurgical techniques for grain refining steel include both mechanical and thermal treatments. Historically, mechanical treatments have been emphasized because of their efficiency in achieving fine grain

size. However thermal treatments have an inherent appeal in that they should yield a more homogeneous product microstructure and do not prohibit the use of the grain refined alloy in welded structures. Hence a major focus of our own research has been on the development of thermal processes which lead to a grain refinement comparable to the best obtainable with mechanical treatments. The results of this research showed that an ultrafine grain size can be established in Fe-Ni alloys through a thermal cycling procedure (described below) which utilizes the phase transformation behavior of the alloy.

There is a final mechanism of toughening which has proven useful in Fe-Ni alloys, based on the possibility of introducing a small quantity of the γ(FCC) phase into the microstructure by heat treating the alloy just within the two-phase ($\alpha + \gamma$) region in the phase diagram. While the beneficial effect of γ on the low temperature toughness of several alloys is well documented[2,3] the specific mechanism responsible for the increase in toughness is not well known. Recent research[4] has however, demonstrated that the γ phase forms as fine grains in grain boundaries, martensite lathe boundaries, and at precipitates in the ferrite phase (Fig. 3), and that the γ phase transforms to α-martensite when the alloy is deformed at low temperature. These observations suggest several possible toughening mechanisms, including a scouring effect of the γ-phase which may remove deleterious species from grain and lathe boundaries (most species are more soluble in the γ than in the α phase and will hence tend to congregate in the γ), a cushioning effect of the more deformable γ which may facilitate the transmission of strain from grain to grain, and a direct contribution from the deformation

associated with the $\gamma \rightarrow \alpha$ transformation to blunt internal flaws or relieve internal stress concentrations (the TRIP toughening mechanism).[5] Recent research[6] has further shown that the beneficial effect of retained austenite on the cryogenic properties of research Fe-Ni alloys is principally due to a lowering of the ductile-brittle transition temperature. When an alloy is tested above T_B the presence of retained austenite may actually decrease its resistance to unstable crack propagation.

III. TREATMENT AND CRYOGENIC MECHANICAL PROPERTIES OF TWO NEW FERRITIC STEELS

The alloy design principles described in the previous section were used to design two new cryogenic steels, of nominal composition Fe-12Ni-0.25Ti and Fe-8Ni-2Mn-0.25Ti. (Typical actual ingot compositions are given in Table I.) The former, which was chronologically the first,[7,8,9] can be processed to have an outstanding combination of strength and toughness at temperatures as low as 4°K (liquid helium temperature) while remaining fully ferritic. The latter,[6] which offers the economic advantage of a lower nickel content, can be processed to have a good combination of cryogenic strength and toughness on addition of a controlled distribution of the austenite (γ) phase. We describe the alloys in turn.

(a) Fe-12Ni-0.25Ti

In the Fe-12Ni-0.25Ti alloy the 12% nickel addition insures a desirable, dislocated α-martensite substructure (Fig. 1) on quenching and also provides phase transformation temperatures and kinetics

favorable for thermal processing to fine grain size. The 0.25Ti addition serves to getter impurity species,[10] principally carbon and oxygen, and combines with nickel to form a fine Ni_3Ti precipitate[11] (Fig. 2) which gives a small increase in yield strength.

Thermal processing to ultrafine grain size is accomplished through the thermal cycling procedure diagramed in Fig. 4, which involves alternate anneals in the austenite (γ) and two-phase ($\alpha + \gamma$) stability fields. The evolution of microstructure during cycling is shown in Fig. 5. The final structure (2B) has ultrafine grain size, with mean grain diameter near 1μm (ASTM #17). The basis of this grain refining procedure is described in reference 8. It may be summarized as follows.

If an Fe-12Ni-0.25Ti alloy is heated continuously from the ferrite (α) to austenite (γ) stability field the $\alpha \rightarrow \gamma$ transformation occurs primarily through a shear transformation mechanism which initiates at a temperature near 673°C and is substantially complete at 715°C. If the alloy is then cooled to room temperature the structure reverts to α through a martensitic transformation. A single cycle of this sort leads to appreciable grain refinement of an annealed alloy (structure 1A in Fig. 5); in a typical experiment alloy grain size was reduced from an initial 40μm (ASTM #6) to ~15μm (ASTM #9). The driving force for grain refinement is believed to be the strain accumulated during the $\alpha \rightarrow \gamma$ shear transformation. A repeat of this simple γ-cycle will give further grain refinement. However, succeeding cycles are less efficient and the grain size stabilizes at ~10μm after 3-4 cycles.

If the 1A structure is subsequently heat treated within the two phase ($\alpha + \gamma$) region at a temperature in the range 600°C-660°C part of

the α phase transforms to γ by a nucleation and growth mechanism. Both the grain boundaries and martensite lathe boundaries of the α serve as perferential nucleation sites, and the 1A structure decomposes into a fine layered structure. On subsequent cooling to room temperature the γ platelets in this structure revert to α, yielding the structure 1B shown in Fig. 5. This structure appears fine grained, but it is not a desirable one for cryogenic toughness. The preferential alignment of adjacent platelets provides easy crack propagation paths along platelet boundaries and hence causes a deterioration in toughness.

To achieve toughness the preferential alignment of grains must be broken up. This is accomplished by simply repeating the two-step heat treating process: an anneal at 730°C, leading to structure 2A, followed by an anneal at 650°C, which establishes the final structure (2B) of fine, non-aligned grains. The alloy 2B is apparently wholly ferritic in structure; no residual austenite has been detected.[8]

The tensile, Charpy Impact, and fracture toughness properties of the grain refined alloy (structure 2B) at 77°K (liquid nitrogen temperature) and at 4-6°K (near liquid helium temperatures) are summarized in Tables II-III. The cryogenic testing techniques employed to obtain this data are described in references 9 and 12. The data is taken from references 6-10. The data are compared to those obtained with the Fe-12Ni-0.25Ti alloy before grain refining (structure 1A) and to those of two commercial cryogenic steels: 9-Ni steel, an Fe-9Ni-1Mn-0.1C ferritic steel with an addition of retained austenite for cryogenic toughness, and 304 stainless steel, an Fe-18Cr-8Ni austenitic alloy. As can be seen from the tables the grain refined Fe-12Ni-0.25Ti alloy

combines the high yield strength of the 9Ni steel (~200 ksi at 4°K) with a fracture toughness (~230 ksi$\sqrt{in}$) in excess of that of the relatively soft 304 stainless steel.

(b) Fe-8Ni-2Mn-0.25Ti

Economic considerations make it highly desirable to duplicate the properties obtained with the Fe-12Ni-0.25Ti alloy using alloys of lower nickel content. To accomplish this two problems must be overcome. First, the ductile-brittle transition temperature tends to increase as the Ni content is lowered.[13] Hence one must anticipate a higher T_B if Ni content is decreased with a given grain size, and must be prepared to utilize other techniques to restore low temperature toughness. Second, as nickel content decreases in an Fe-Ni alloy the phase transformation temperatures rise, a trend due principally to the increase in the equilibrium transformation temperatures shown in the schematic phase diagram (Fig. 4). As the transformation temperatures rise the heat treating temperatures needed for grain refinement by thermal cycling increase, grain growth becomes more significant, and the grain refinement process is less efficient. Hence an ultrafine grain size is more difficult to achieve.

To overcome these problems we are investigating simultaneous modifications in alloy composition and processing. Initial success has been obtained with an alloy of nominal composition Fe-8Ni-2Mn-0.25Ti. The addition of manganese principally serves to lower the transition temperatures in the alloy and permit grain refinement through thermal cycling, though there are experimental indications that the manganese

may contribute a decrease in T_B. A further depression in T_B is accomplished by introducing a controlled distribution of retained austenite (γ).

The processing sequence for the Fe-8Ni-2Mn-0.25Ti alloy[6] is shown schematically in Fig. 6. The first step is an annealing treatment to remove the deformation strain introduced during the previous forging process. The next four steps (1A-2B) are a grain refinement sequence, essentially identical to that used for the 12Ni alloy. The final step incorporates a distribution of retained austenite, principally in the grain boundaries. Approximately 5% in volume of retained austenite was found in the structure 2BR by the X-ray diffraction analysis. The microstructures are shown in Fig. 7. It is fine grained, though the grains appear slightly larger and slightly less uniform than was the case for the 12Ni alloy. The form and distribution of retained austenite are illustrated in the electron micrograph of Fig. 8, which also reveals the substructure of matrix grains.

The tensile properties of the Fe-8Ni-2Mn-0.25Ti alloy and its Charpy impact energy are included in Table II. As is apparent from this data, the alloy retains outstanding impact toughness to liquid helium temperature. The variation of T_B with processing is illustrated in Fig. 9. The grain refinement process suppresses T_B, as measured by the Charpy impact energy, from +44°C to -118°C. The addition of retained austenite further suppresses T_B to below liquid helium temperature. Cryogenic fracture toughness tests on this alloy are currently in progress.

IV. CONCLUSION

The research reviewed here has shown that metallurgical techniques can be used to design alloys which retain high toughness at high strength to liquid helium temperature and below. While the alloys described here are laboratory alloys, the results indicate that new materials can be developed to meet future needs for high strength, high toughness steels for advanced cryogenic systems.

ACKNOWLEDGMENT

The authors appreciate the assistance of S. K. Hwang, Sheree H. Wen and B. W. Whitaker for helpful discussions and research results. This work was supported by the Office of Naval Research under Contract No. N0014-69-A-1062, NR 031-762, and by the Atomic Energy Commission through the Inorganic Materials Research Division of the Lawrence Berkeley Laboratory.

REFERENCES

1. See, for example, A. H. Cottrell, The Mechanical Properties of Matter (J. Wiley, New York, 1969), Chapter 11.

2. C. W. Marschall, R. F. Hehemann and A. R. Troiano, Trans. ASM 55, 135 (1962).

3. S. Nagashima, T. Ooka, S. Sekino, H. Mimura, T. Fujishima, S. Yano, and H. Sakurai, Trans. ISIJ 11, 402 (1971).

4. S. K. Hwang and J. W. Morris, Jr., Met. Trans. (submitted).

5. V. F. Zackay, E. R. Parker, D. Fahr, and R. Busch, Trans. ASM 60, 252 (1967).

6. S. Jin, S. K. Hwang, and J. W. Morris, Jr., Met. Trans. (submitted).

7. S. Jin, J. W. Morris, Jr., and V. F. Zackay, Advances in Cryogenic Engineering, Vol. 19, p. 379 (1974).

8. S. Jin, J. W. Morris, Jr., and V. F. Zackay, Met. Trans. (in press).

9. S. Jin, S. K. Hwang, and J. W. Morris, Jr., Met. Trans. (submitted).

10. W. C. Leslie, R. J. Sober, S. G. Babcock, and S. J. Green, Trans. ASM 62, 690 (1969).

11. G. R. Speich, Trans. AIME 227, 1426 (1963).

12. S. Jin, W. A. Horwood, J. W. Morris, Jr., and V. F. Zackay, Advances in Cryogenic Engineering, Vol. 19, p. 373 (1974).

13. N. S. Stoloff, Fracture, edited by H. Liebowitz (Academic Press, 1969), Vol. 6, p. 1.

Table I. Typical Chemical Compositions of Laboratory Ingots (wt. percent).

	Fe	Ni	Mn	Ti	C	N	S	P
Fe-12Ni-0.25Ti	Bal	12.07	-	0.26	0.001	0.014	0.004	0.003
Fe-8Ni-2Mn-0.25Ti	Bal	8.03	1.97	0.17	0.001	0.001	0.006	0.001

Table II. Cryogenic Tensile and Impact Properties

	Alloy	Y.S.* ksi	U.T.S. ksi	Elong. pct.	R.A. pct.	Charpy Energy ft-lb
77°K	Fe-12Ni-0.25Ti (1A)	134	142	31.1	73.8	154
	Fe-12Ni-0.25Ti (2B)	149	154	26.8	72.1	115
	9-Ni steel	146	172	29.6	66.8	92
	304 stainless	81	235	47.3	65.6	128
	Fe-8Ni-2Mn-0.25Ti (AN)	131	149	22.5	44.9	4
	Fe-8Ni-2Mn-0.25Ti (2BR)	124	148	36.0	75.1	163
4.2°K	Fe-12Ni-0.25Ti (1A)	182	207	23.8	72.9	55
	Fe-12Ni-0.25Ti (2B)	195	219	19.3	69.8	99
	9-Ni steel	208	231	21.2	59.1	75
	304 stainless	105	270	41.6	52.7	130
	Fe-8Ni-2Mn-0.25Ti (AN)					below 4
	Fe-8Ni-2Mn-0.25Ti (2BR)					137

*At 77°K, 0.2 percent offset yield strengths were taken. At 4.2°K, the first discontinuous yield points were used.

†To convert to SI units, 1 ksi = 689 × 10^6 N/m^2, and 1 ft-lb = 1.36 Nm.

Table III. Fracture Toughness at Cryogenic Temperatures

	K_{IC} at 77°K $ksi\sqrt{in}$	K_{IC} at 6°K $ksi\sqrt{in}$
Fe-12Ni-0.25Ti (1A)	187*	75 (valid K_{IC})
9-Ni steel	168*	73 (valid K_{IC})
Fe-12Ni-0.25Ti (2B)	307*	232*
304 stainless	213*	168*

*Values calculated using Equivalent Energy concept.

†Compact Tension fracture toughness specimens of 0.7 in. thickness were tested in accordance with ASTM specification.

††To convert to SI units, 1 $ksi\sqrt{in} = 1.09 \times 10^6$ $N/m^2 \cdot \sqrt{m}$.

XBB 7411-8785

Fig. 1. Transmission electron micrograph showing dislocated martensite in an Fe-12Ni alloy.

XBB 7411-8786

Fig. 2. Transmission Electron micrograph showing Ni_3Ti precipitates in an Fe-12Ni-0.25Ti alloy.

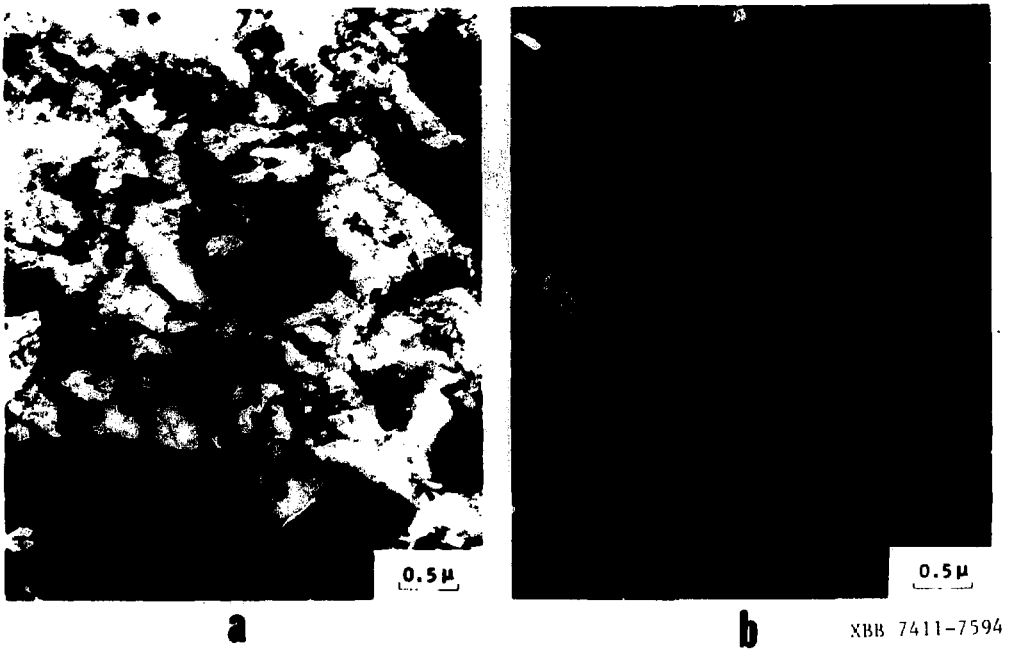

Fig. 3. Transmission electron micrographs of a heat treated Fe-12Ni-0.25Ti alloy containing introduced austenite phase. (a) Bright field image showing substructure; (b) Dark field image from the $(200)_\gamma$ reflection. The bright areas in the dark field image are properly oriented austenite grains.

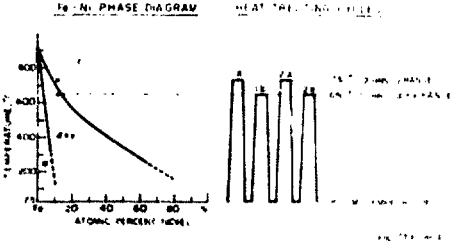

Fig. 4. Thermal cycling procedure of grain refinement in an Fe-12Ni-0.25Ti alloy.

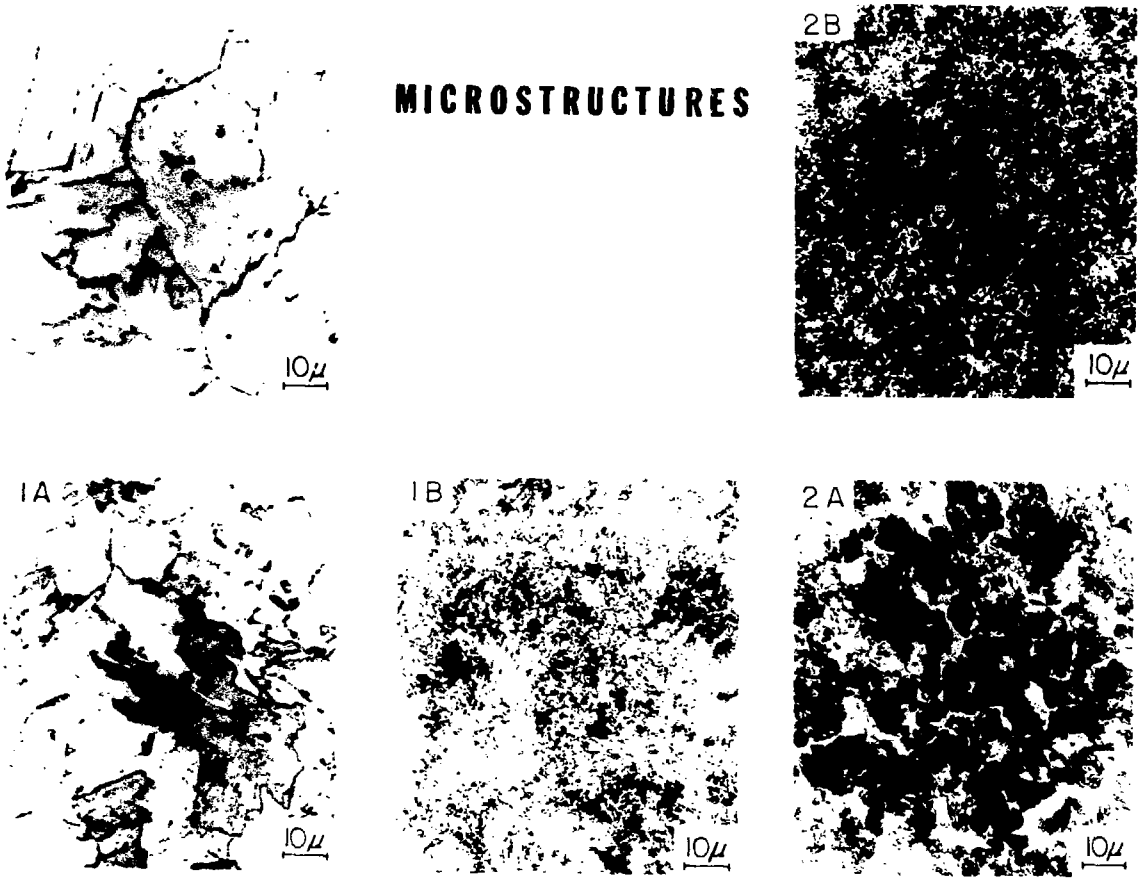

Fig. 5. Change of optical microstructures of the Fe-12Ni-0.25Ti alloy. XBB 739-5684

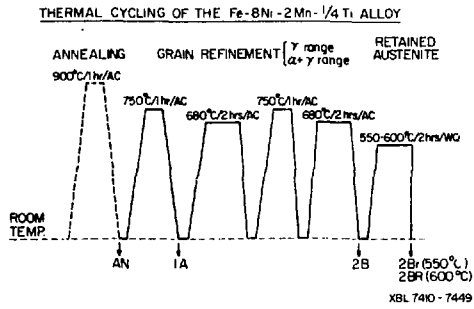

Fig. 6. Thermal cycling procedure for grain refinement and introduction of austenite in an Fe-8Ni-2Mn-0.25Ti alloy.

MICROSTRUCTURES

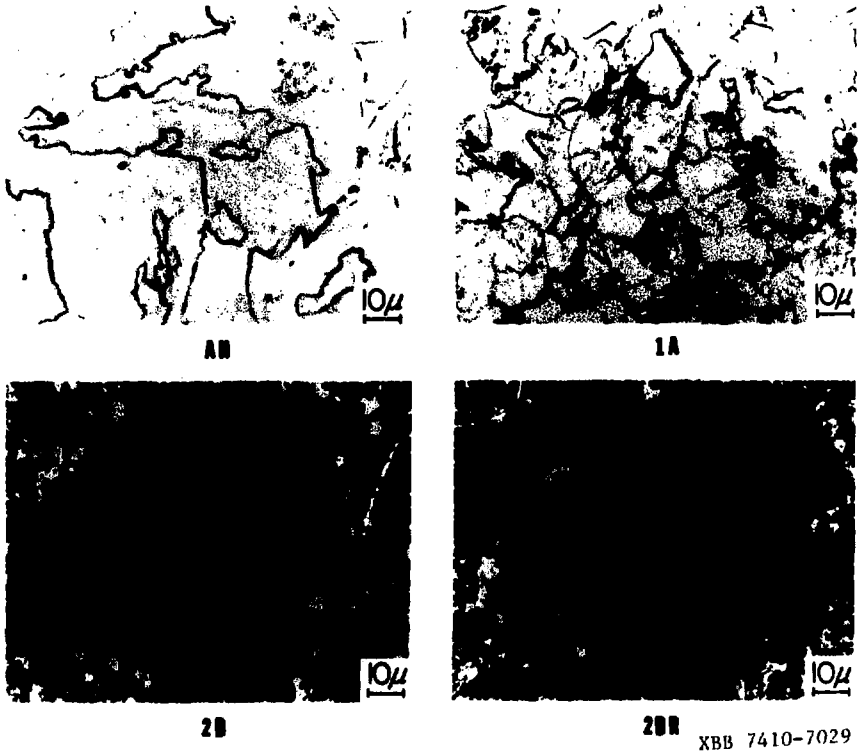

Fig. 7. Microstructures of an Fe-8Ni-2Mn-0.25Ti alloy.

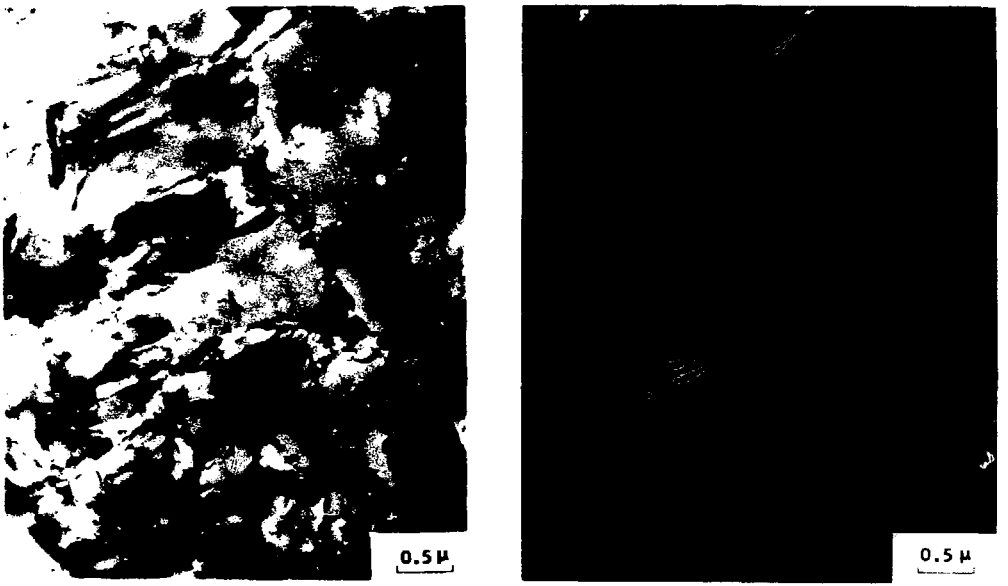

XBB 7411-7592

Fig. 8. Transmission electron micrographs of a heat treated Fe-8Ni-2Mn-0.25Ti alloy. (a) Bright field image showing substructure. (b) Dark field image from the $(200)_\gamma$ reflection. The bright areas in the dark field image are properly oriented austenite grains.

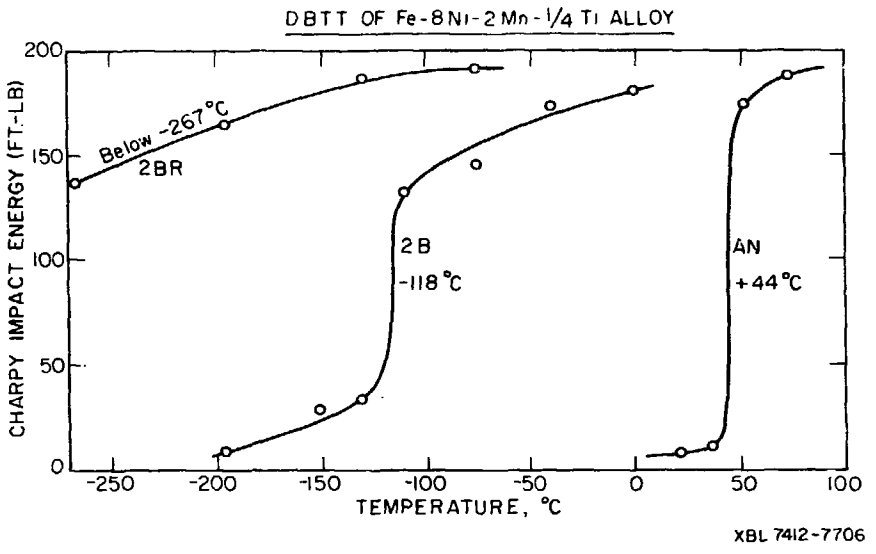

Fig. 9. Suppression of the ductile-brittle transition temperature by grain refinement and retained austenite.